



Published in final edited form as:

*Nanoscale*. 2014 August 7; 6(15): 8873–8877. doi:10.1039/c4nr02097a.

## Environmentally Responsive Histidine-Carboxylate Zipper Formation between Proteins and Nanoparticles

Rubul Mout, Gulen Yesilbag Tonga, Moumita Ray, Daniel F Moyano, and Vincent M. Rotello  
Department of Chemistry, University of Massachusetts, 710 North Pleasant Street, Amherst, Massachusetts 01003, USA, Fax: (+1)413-545-208

Vincent M. Rotello: rotello@chem.umass.edu

### Abstract

Interfacing synthetic materials with biomacromolecules provides new systems for biological applications. We report the creation of a reversible multivalent supramolecular "zipper" recognition motif between gold nanoparticles and proteins. In this assembly, carboxylate-functionalized nanoparticles interact strongly with oligohistidine tags. This interaction can be tuned through His-tag length, and offers unique binding profiles based on the pH and electrolyte concentration of the medium.

### Introduction

Tailoring molecular recognition between synthetic materials and biomolecules provides a versatile strategy for creating bioconjugate systems.<sup>1</sup> A variety of supramolecular approaches have been devised to interface synthetic and biological systems for diverse applications.<sup>2</sup> However, using these systems in physiological environments such as is challenging, where high concentrations of proteins and other biomolecules compete for interaction.

Co-engineering of biomolecules and synthetic materials and provides a strategy for generating high affinity and reversible molecular interactions.<sup>3</sup> Inspiration for this codesign can be obtained from Nature: naturally occurring molecular zippers, including duplex DNA<sup>4</sup> and leucine zippers<sup>5</sup> exhibit robust multivalent reversible interactions in intracellular conditions. Microtubules polymerize and de-polymerize through the formation of specific molecular zippers.<sup>6</sup> This multivalent motif<sup>7</sup> has been used to create synthetic molecular duplexes<sup>8</sup> through non-covalent interactions including electrostatic interactions,<sup>9</sup> hydrogen bonding,<sup>10</sup>  $\pi$ - $\pi$  interactions,<sup>11</sup> and van der Waals forces to generate zippers.<sup>12</sup>

Multivalency is a key structural prerequisite for zipper motifs. Nanomaterials offers molecular scaffolds that can be engineered to present multivalent recognition elements.<sup>13</sup> Gold nanoparticles (AuNPs) provide a particularly versatile platform for biomolecular recognition,<sup>14</sup> and have been interfaced with proteins for a wide variety of applications.<sup>15</sup>

Correspondence to: Vincent M. Rotello, rotello@chem.umass.edu.

†Electronic Supplementary Information (ESI) available: Nanoparticle characterizations- i.e. Zeta potential, DLS, and TEM and GFP sequence. See DOI: 10.1039/b000000x/

The AuNP surface can be readily engineered to feature recognition elements. Additionally, AuNPs can be generated with sizes commensurate to proteins, providing surface complementarity for recognition while maintaining effective biological function.<sup>16</sup>

The metal ion-mediated oligohistidine-nitrilotriacetate recognition motif has been widely employed to capture proteins using nanomaterials.<sup>17</sup> We hypothesized that the oligohistidine cationic tail<sup>18</sup> used in this strategy could be employed as a zipper component for interaction with nanomaterials. In this report, we demonstrate a reversible molecular zipper between His-tagged proteins and carboxylate functionalized AuNPs. This zipper exhibits high affinity binding in physiologically relevant environments, including serum conditions. The system is also environmentally responsive, with binding dictated by solution pH. This new recognition motif presents opportunities for engineering specific molecular interactions between synthetic and biomolecules.

## Results and discussion

The host nanoparticle was provided by AuNPs (2nm core diameter) functionalized with anionic ligands (AuNP-COOH) that can interact with proteins without denaturation.<sup>19</sup> We next explored the interaction of these inherently multivalent carboxylate particles with a family of His-tagged green fluorescent proteins (GFP)<sup>20</sup> (Fig. 1). We cloned and purified three eGFP<sup>21</sup> variants carrying different length of N-terminal His-tags: one His (1×His-GFP), six His (6×His-GFP), and twelve His (12×His-GFP) to determine the required number of interactions. These proteins were all anionic, with predicted pI values of 5.8, 6.1, and 6.5, respectively.

The binding efficiency of AuNP-COOH with the His-tagged GFPs was quantified through fluorescence titration,<sup>22</sup> utilizing the quenching properties of the AuNP.<sup>23</sup> At low ionic strength (5 mM phosphate buffer, PB) AuNP-COOH bound both 12×His-GFP and 6×His-GFP with high affinity (Fig. 2a). The binding constant ( $K_S$ ) values for 12×His-GFP ( $K_S = 2.95 \pm 0.6 \times 10^7 \text{ M}^{-1}$ ) was ~3-fold higher than that of 6×His-GFP ( $K_S = 7.8 \pm 0.38 \times 10^6 \text{ M}^{-1}$ ), indicating that multivalency is crucial for zipper formation. Interestingly, more GFPs bound to each nanoparticle for 12×His-GFP ( $n = 11.6 \pm 0.8$ ) than for 6×His-GFP ( $n = 4.7 \pm 1$ ), potentially due to decreased secondary repulsion between the anionic GFPs.<sup>24</sup> No observable binding was observed with 1×His-GFP, demonstrating that specific zipper formation was required for interaction.

The pragmatic use of non-covalent bioconjugates requires high affinity interactions at physiological ionic strength. In previous studies, electrostatic interactions between nanoparticles and proteins were fully disrupted at quite low salt concentrations, typically 10–50 mM salt.<sup>25</sup> In contrast, high binding affinities were observed between AuNP-COOH and both 12×His-GFP ( $K_S = 1.3 \pm 0.16 \times 10^7 \text{ M}^{-1}$ ), and 6×His-GFP ( $K_S = 1.4 \pm 0.2 \times 10^6 \text{ M}^{-1}$ ) in PBS buffer (150 mM NaCl in 5 mM PB, pH 7.4) (Fig. 2b). Notably, a larger  $n$  value was observed for 12×His-GFP, similar to the one at low (5 mM) electrolyte concentration.

## Reversible zipper formation at physiologically relevant conditions

One of the key advantages of supramolecular bioconjugates is their ability to respond to environmental changes. pH is an important biological parameter. For example, normal tissues have a pH of 7.4, while tumor tissues have lower pH (~6 to 7).<sup>26</sup> Additionally, pH decreases through the endosomal/lysosomal pathways inside cells, reaching a pH of ~4.8.<sup>27</sup> In our system, the histidine tag in GFPs offers a potentially pH-switchable recognition scaffold. To explore this possibility, we investigated the pH and ionic strength dependent reversibility of the carboxylate-histidine zipper formation. Both 12×His-GFP and 6×His-GFP interacted strongly with AuNP-COOH below pH ~7.5 at physiological salt concentration (PBS). Significantly, above pH ~7.5 the carboxylate-histidine zipper disassembled, releasing the GFP from the nanoparticles surface (Fig. 3a and 3b). As expected, 1×His-GFP did not interact with nanoparticles at any condition (Fig. 3c). Taken together, these studies demonstrated the pH response of the zipper motif.

## Reversible zipper formation in serum conditions

*In vivo* applications including protein and gene delivery require specific and reversible interactions between synthetic carrier materials and the cargo molecules in serum.<sup>28</sup> Serum presents a complex competitive chemical environment featuring a high (~1 mM) concentration of protein,<sup>29</sup> making it challenging to engineer effective recognition motifs. We parametrically investigated the serum concentration and pH dependent reversibility of the carboxylate-histidine zipper. At pH <7.5 and at 10% serum (cell culture condition), 12×His-GFP exhibited a high affinity binding towards AuNP-COOH (Fig. 4a). Significantly, in 55% serum condition (*in vivo* condition) at pH 7.5 there was substantial binding between AuNP-COOH and 12×His-GFP (Fig. 4c). While the binding isotherm is complex, considerable binding was observed at high nanomolar concentrations. In contrast, 6×His-GFP did not bind with AuNP-COOH at any serum condition under investigation (Fig. 4b), indicating that a high degree of multivalency is crucial for carboxylate-histidine zipper formation in complex biological environments.

## Conclusions

In summary, we have tailored a molecular zipper based on multivalent carboxylate-histidine interactions through co-engineering of the AuNP surface and proteins. The carboxylate-histidine zipper exhibited high affinity interactions under physiologically relevant conditions that were pH responsive, making these systems attractive starting points for delivery and imaging applications. In a broader context, these studies demonstrate how co-engineering of biomolecules and nanoparticles can be used to generate bioconjugates with new and useful properties..

## Experimental section

### Materials and methods

**Cloning and over expression of green fluorescent proteins (GFPs)**—Genetic engineering manipulation and protein expression were done according to standard protocols. (a) To generate 1×His-GFP, a constitutive expression vector (pUCCB-ntH6-eGFP) was

purchased from Addgene (plasmid id- 32557).<sup>30</sup> For the sake of purification, a 6×His tag was placed on the N-terminus of 1×His-GFP, upstream of a thrombin cleavage site. (b) 6×His-GFP expression vector (pET21-d-GFP) was obtained from Novagen. (c) 12×His-GFP was generated by incorporating twelve histidines in the N-terminus of GFP. Briefly, using GFP as the template, PCR was performed with the following primers. Subsequently, the PCR product was digested (using *Bam*HI and *Hind*III restriction enzymes) and inserted into pQE80 vector, downstream of nucleotides for six histidine tag to construct pQE80-12×His-GFP expression vector. Successful cloning was confirmed by DNA sequencing. Forward primer: 5'- ACGATGGATCCCACCATCACCAT -3' Reverse primer: 5'- GTGACAAGCTTTTACTTGTACAGCTC -3'

To produce recombinant proteins, plasmids carrying 1×His-GFP, 6×His-GFP, or 12×His-GFP was transformed into *Escherichia coli* BL21(DE3) strain. A transformed colony was picked up to grow small cultures in 50 mL 2×YT media at 37 °C for overnight. The following day, 15 mL of grown culture was inoculated into one liter 2×YT media and allowed to grow at 37 °C until OD reaches 0.6. At this point, the protein expression was induced by adding isopropyl-b-D-thiogalactopyranoside (IPTG; 1 mM final concentration) at 25 °C. After 16 hours of induction, the cells were harvested and the pellets were lysed using a microfluidizer. His-tagged fluorescent proteins were purified from the lysed supernatant using HisPur cobalt columns. The integrity and the purity of native protein were determined by 12% SDS-PAGE gel.

1×His-GFP was cleaved from its 6×His tag using thrombin-agarose beads (Thrombin CleanCleave™ Kit, Sigma-Aldrich) as described in the instruction manual. After the cleavage, 1×His-GFP was passed through a HisPur cobalt column to remove the cleaved 6×His tag. Further, the residual 6×His was removed by a 10KD-MWCO (molecular weight cut off) filter.

**Synthesis and characterization of nanoparticles**—Carboxylate functionalized gold nanoparticles (AuNP-COOH) were synthesized according to a previous report.<sup>31</sup> Briefly, Brust-Schiffrin two-phase synthesis was used to synthesize pentanethiol-coated AuNPs with core diameter ~2 nm.<sup>32</sup> The Murray place-exchange method was followed to obtain AuNP-COOH.<sup>33</sup> The monolayer protected nanoparticles were re-dispersed in water. The excess ligand/pentanethiol were removed by dialysis using a 10,000 MWCO snake-skin membrane. The final concentration was measured by UV spectroscopy at 502 nm. To assess their quality, the nanoparticles were characterized by Zeta potential (surface charge), Dynamic Light Scattering (DLS) (hydrodynamic radius), and Transmission Electron Microscopy (TEM) (core size) as shown in Fig. S1.

**Fluorescence titration**—Fluorescence titration experiments between nanoparticles and GFPs were carried out as described previously.<sup>34</sup> Briefly, the change of fluorescence intensity of GFPs at 510 nm was measured with an excitation wavelength of 475 nm at various concentrations of nanoparticles from 0 to 400 nM on a Molecular Devices SpectraMax M3 microplate reader (at 25 °C). Quenching of fluorescence intensity arising from 100 nM GFP was observed with increasing nanoparticle concentration. Nonlinear

least-squares curve fitting analysis was carried out to estimate the binding constant ( $K_S$ ) and association stoichiometry ( $n$ ,  $[GFP]/[AuNP-COOH]$ ) using a one site binding model.<sup>21</sup>

For the pH and salt dependent interactions (fluorescence titrations) between nanoparticles and GFPs, the concentration of GFP chosen was 100 nM for each study. The concentrations of AuNP-COOH used for the titrations were 400 nM. The fluorescence intensity for each study was normalized against the intensity of GFP without nanoparticles at their respective pH and salt (NaCl in 5 mM PB) concentration. The titrations were carried out in triplicates, and repeated at least twice with different batches of nanoparticles.

Similar fluorescence titrations were performed for the serum concentration and pH dependent interactions between AuNP-COOH and His-tagged GFPs. Both the nanoparticle (400 nM) and GFP (100 nM) concentrations were kept fixed, varying the serum percentage and pH of the solutions. In a typical experiment, AuNP-COOH/GFP complexes were made first, incubated at dark for 10 minutes, then the required serum amount was added to the complexes, followed by immediate shaking for 30 seconds. Fluorescence reading was taken after 30 minutes of incubation.

## Supplementary Material

Refer to Web version on PubMed Central for supplementary material.

## Acknowledgements

This research was funded by NIH (GM077173 and EB014277), and NSF instrumentation (MRSEC, DMR-0820506).

## Notes and references

1. (a) Lehn JM. *Science*. 2002; 295:2400. [PubMed: 11923524] (b) Zhang J, Landry MP, Barone PW, Kim JH, Lin S, Ulissi ZW, Lin D, Mu B, Boghossian AA, Hilmer AJ, Rwei A, Hinckley AC, Kruss S, Shandell MA, Nair N, Blake S, Sen F, Sen S, Croy RG, Li D, Yum K, Ahn JH, Jin H, Heller DA, Essigmann JM, Blankschtein D, Strano MS. *Nat. Nanotechnol.* 2013; 8:959. [PubMed: 24270641]
2. (a) Ostuni E, Yan L, Whitesides GM. *Colloids Surf. B.* 1999; 15:3.(b) Whaley SR, English DS, Hu EL, Barbara PF, Belcher AM. *Nature*. 2000; 405:665. [PubMed: 10864319] (c) Seeman NC, Belcher AM. *Proc. Natl. Acad. Sci. U S A.* 2002; 99:6451. [PubMed: 11880609] (d) Niemeyer CM. *Angew. Chem. Int. Ed.* 2001; 40:4128.(e) Cooper W, Waters ML. *Curr. Opin. Chem. Biol.* 2005; 9:627. [PubMed: 16257571] (e) Chen I, Ting AY. *Curr. Opin. Biotechnol.* 2005; 16:35. [PubMed: 15722013] (f) Mout R, Moyano DF, Rana S, Rotello VM. *Chem. Soc. Rev.* 2012; 41:2539. [PubMed: 22310807]
3. Kostiaainen MA, Hiekkataipale P, Laiho A, Lemieux V, Seitsonen J, Ruokolainen J, Ceci P. *Nat. Nanotechnol.* 2013; 8:52. [PubMed: 23241655]
4. Weaver, RF. *Molecular Biology*. 5th ed. McGraw-Hill; 2011.
5. (a) Nir E, Kleinermanns K, de Vries MS. *Nature*. 2000; 408:949. [PubMed: 11140676] (b) Landschulz WH, Johnson PF, McKnight SL. *Science*. 1988; 240:1759. [PubMed: 3289117] (c) Munro OQ, du Toit K, Drewes SE, Crouch NR, Mulholland DA. *New J. Chem.* 2006; 30:197.
6. (a) Kikkawa M, Metlagel Z. *Cell*. 2006; 127:1302. [PubMed: 17190594] (b) Sandblad L, Busch KE, Tittmann P, Gross H, Brunner D, Hoenger A. *Cell*. 2006; 127:1415. [PubMed: 17190604]
7. Levine PM, Carberry TP, Holub JM, Kirshenbaum K. *Med. Chem. Commun.* 2013; 4:493.
8. (a) Bisson AP, Carver FJ, Hunter CA, Walthot JP. *J. Am. Chem. Soc.* 1994; 116:10292.(b) Zeng H, Yang X, Flowers RA, Gong B. *J. Am. Chem. Soc.* 2002; 124:2903. [PubMed: 11902880] (c) Yang

- XW, Hua FJ, Yamato K, Ruckenstein E, Gong B, Kim W, Ryu CY. *Angew. Chem. Int. Ed.* 2004; 43:6471.(d) Wu L, McElheny D, Huang R, Keiderling TA. *Biochemistry.* 2009; 48:10362. [PubMed: 19788311] (e) Hwang S, Hilty C. *J. Phys. Chem. B.* 2011; 115:15355. [PubMed: 22040105] (f) Culik RM, Jo H, DeGrado WF, Gai F. *J. Am. Chem. Soc.* 2012; 134:8026. [PubMed: 22540162]
9. Diss ML, Kennan AJ. *Org. Lett.* 2008; 10:3797. [PubMed: 18693746]
  10. Spencer R, Chen KH, Manuel G, Nowick JS. *Eur. J. Org. Chem.* 2013; 3523
  11. Waters ML. *Biopolymers.* 2004; 76:435. [PubMed: 15478139]
  12. (a) Bisson AP, Carver FJ, Eggleston DS, Haltiwanger RC, Hunter CA, Livingstone DL, McCabe JF, Rotger C, Rowan AE. *J. Am. Chem. Soc.* 2000; 122:8856.(b) Kim HW, Jung J, Han M, Lim S, Tamada K, Hara M, Kawai M, Kim Y, Kuk Y. *J. Am. Chem. Soc.* 2011; 133:9236. [PubMed: 21591706]
  13. (a) Rana S, Bajaj A, Mout R, Rotello VM. *Adv. Drug. Deliv. Rev.* 2012; 64:200. [PubMed: 21925556] (b) Drechsler U, Erdogan B, Rotello VM. *Chemistry.* 2004; 10:5570. [PubMed: 15372582] (c) Giljohann DA, Seferos DS, Daniel WL, Massich MD, Patel PC, Mirkin CA. *Angew. Chem. Int. Ed. Engl.* 2010; 49:3280. [PubMed: 20401880]
  14. Daniel MC, Astruc D. *Chem. Rev.* 2004; 104:293. [PubMed: 14719978]
  15. (a) Walkey CD, Chan WC. *Chem. Soc. Rev.* 2012; 41:2780. [PubMed: 22086677] (b) Mout R, Rotello VM. *Isr. J. Chem.* 2013; 53:521.
  16. Rosi NL, Mirkin CA. *Chem. Rev.* 2005; 105:1547. [PubMed: 15826019]
  17. (a) Abad JM, Mertens SF, Pita M, Fernández VM, Schiffrin DJ. *J. Am. Chem. Soc.* 2005; 127:5689. [PubMed: 15826209] (b) De M, Rana S, Rotello VM. *Macromol. Biosci.* 2009; 9:174. [PubMed: 19127602] (c) Boeneman K, Mei BC, Dennis AM, Bao G, Mattoussi JRH, Medintz IL. *J. Am. Chem. Soc.* 2009; 131:3828. [PubMed: 19243181]
  18. Marti DN, Bosshard HR. *J. Mol. Biol.* 2003; 330:621. [PubMed: 12842476]
  19. (a) Bayraktar H, You CC, Rotello VM, Knapp MJ. *J. Am. Chem. Soc.* 2007; 129:2732. [PubMed: 17309259] (b) Fischer NO, Verma A, Goodman CM, Simard JM, Rotello VM. *J. Am. Chem. Soc.* 2003; 125:13387. [PubMed: 14583034] (c) Hong R, Emrick T, Rotello VM. *J. Am. Chem. Soc.* 2004; 126:13572. [PubMed: 15493887]
  20. Tsien RY. *Annu. Rev. Biochem.* 1998; 67:509. [PubMed: 9759496]
  21. Cormack BP, Valdivia RH, Falkow S. *Gene.* 1996; 173:33. [PubMed: 8707053]
  22. You CC, De M, Han G, Rotello VM. *J. Am. Chem. Soc.* 2005; 127:12873. [PubMed: 16159281]
  23. (a) Bajaj A, Rana S, Miranda OR, Yawe JC, Jerry DJ, Bunz UHF, Rotello VM. *Chem. Sci.* 2010; 1:134.(b) De M, Rana S, Akpınar H, Miranda OR, Arvizo RR, Bunz UH, Rotello VM. *Nat. Chem.* 2009; 1:461. [PubMed: 20161380]
  24. Torrens F, Castellano G. *J. Cheminform.* 2010; 2(Suppl 1):P12.
  25. (a) Wang L, Wang H, Yuan L, Yang W, Wu Z, Chen H. *J. Mater. Chem.* 2011; 21:13920.(b) Peng ZG, Hidajat K, Uddin MS. *J. Colloid Interface Sci.* 2004; 271:277. [PubMed: 14972603]
  26. (a) Tannock IF, Rotin D. *Cancer Res.* 1989; 49:4373. [PubMed: 2545340] (b) Helmlinger G, Yuan F, Dellian M, Jain RK. *Nat. Med.* 1997; 3:177. [PubMed: 9018236]
  27. Sorkin A, Von Zastrow M. *Nat. Rev. Mol. Cell Biol.* 2002; 3:600. [PubMed: 12154371]
  28. Tang R, Kim CS, Solfiell DJ, Rana S, Mout R, Velázquez-Delgado EM, Chompoosor A, Jeong Y, Yan B, Zhu ZJ, Kim C, Hardy JA, Rotello VM. *ACS Nano.* 2013; 7:6667. [PubMed: 23815280]
  29. Adkins JN, Varnum SM, Auberry KJ, Moore RJ, Angell NH, Smith RD, Springer DL, Pounds JG. *Mol. Cell Proteomics.* 2002; 1:947. [PubMed: 12543931]
  30. Vick JE, Johnson ET, Choudhary S, Bloch SE, Lopez-Gallego F, Srivastava P, Tikh IB, Wawrzyn GT, Schmidt-Dannert C. *Appl. Microbiol. Biotechnol.* 2011; 92:1275. [PubMed: 22033566]
  31. Hong R, Emrick T, Rotello VM. *J. Am. Chem. Soc.* 2004; 126:13572. [PubMed: 15493887]
  32. (a) Kanaras AG, Kamounah FS, Schaumburg K, Kiely CJ, Brust M. *Chem. Commun.* 2002; 20:2294.(b) Brust M, Walker M, Bethell D, Schiffrin DJ, Whyman R. *J. Chem. Soc. Chem..* 1994; 801
  33. Templeton AC, Wuelfing MP, Murray RW. *Acc. Chem. Res.* 2000; 33:27. [PubMed: 10639073]

34. Rana S, Singla AK, Bajaj A, Elci SG, Miranda OR, Mout R, Yan B, Jirik FR, Rotello VM. ACS Nano. 2012; 6:8233. [PubMed: 22920837]

Author Manuscript

Author Manuscript

Author Manuscript

Author Manuscript

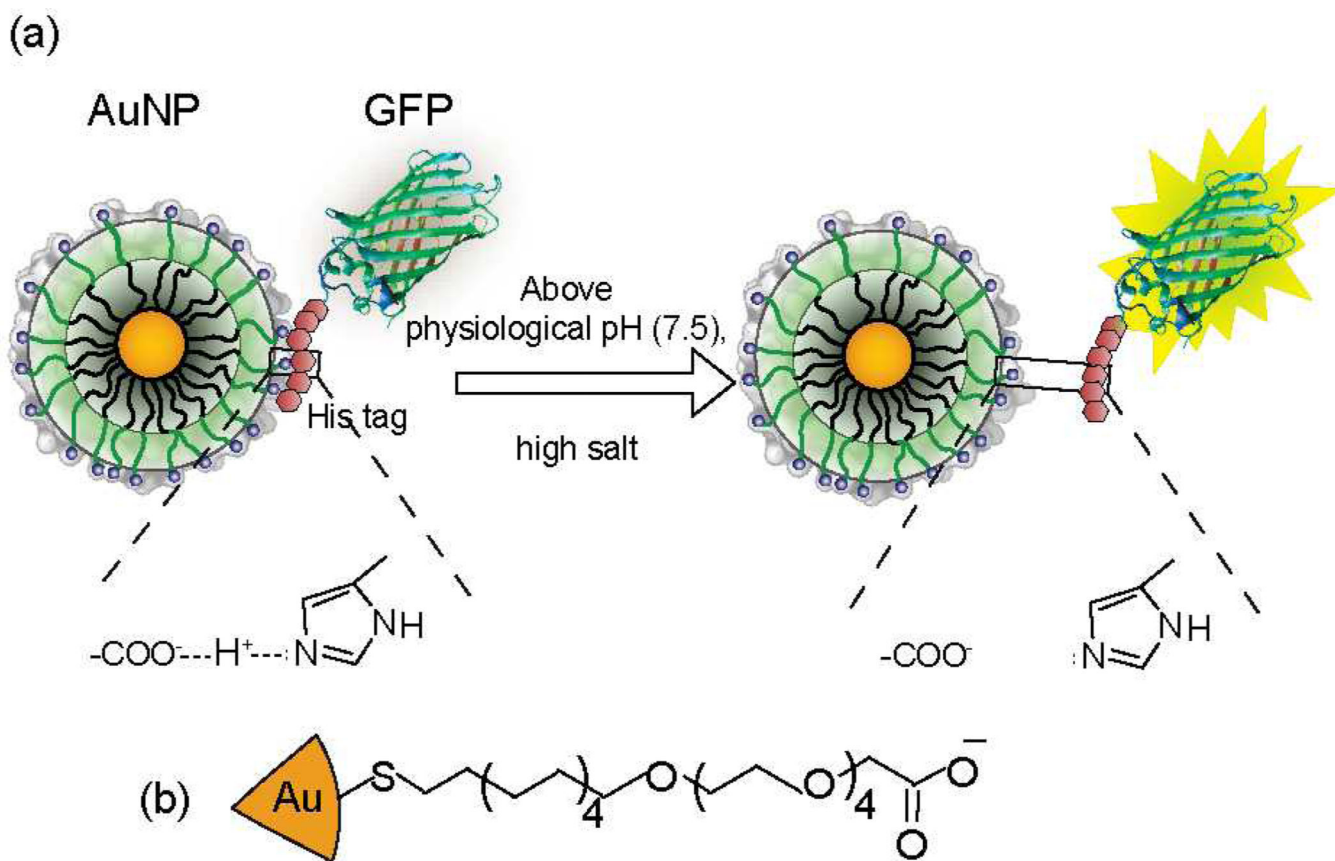


**Fig. 1.**  
 (a) Zipper formation between AuNP-COOH and N-terminus oligohistidine-tagged GFPs through carboxylate-histidine interaction (b) The chemical structure of 2 nm gold core nanoparticle AuNP-COOH.



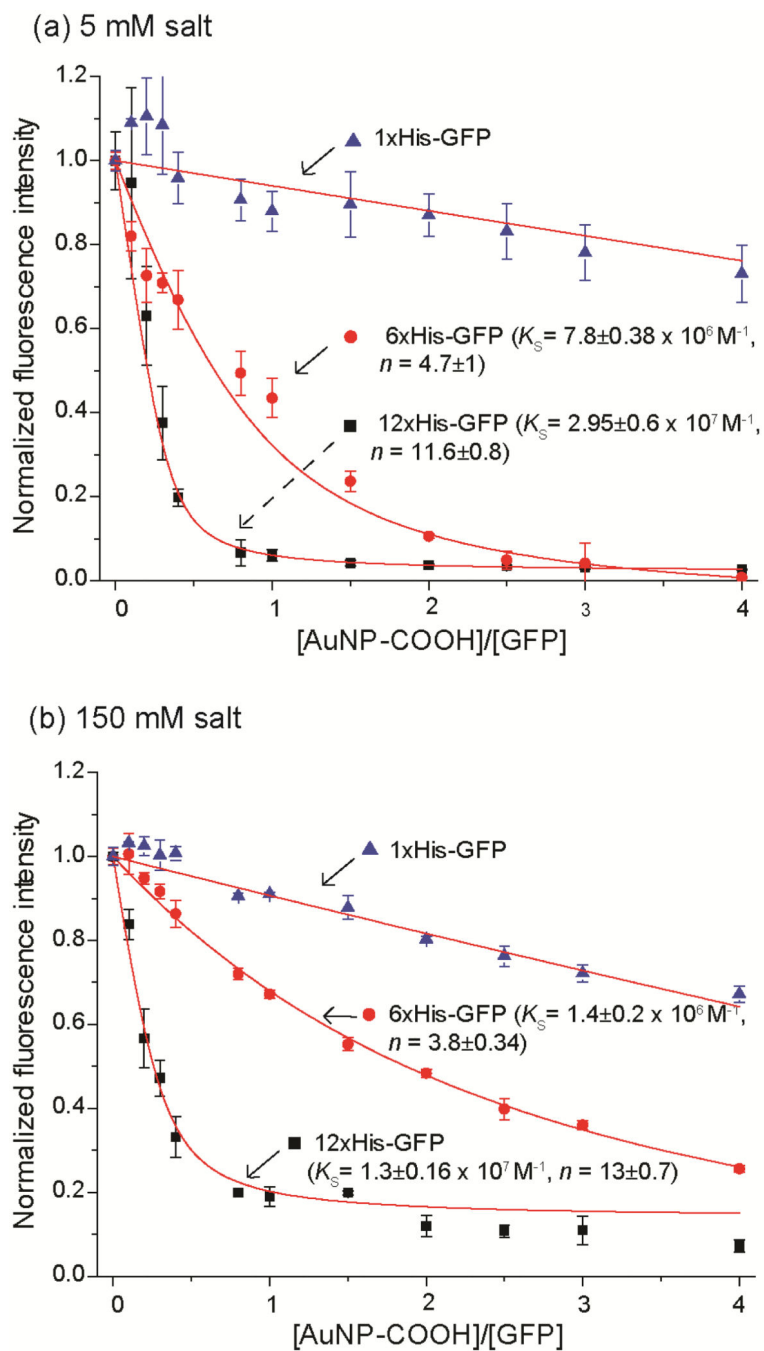
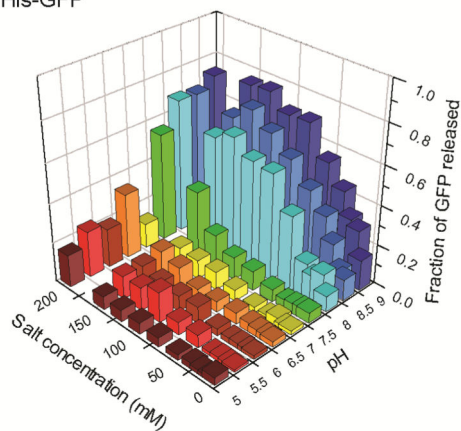
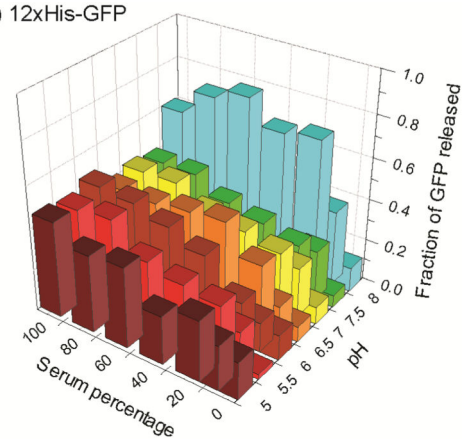


**Fig. 2.** The interaction of AuNP-COOH with His-tagged GFP variants. Fluorescence ( $\lambda_{\text{ex}}=475 \text{ nm}$ ,  $\lambda_{\text{em}}=510 \text{ nm}$ ) titrations between nanoparticles and GFPs (100 nM) in (a) 5 mM phosphate buffer (PB), and (b) PBS buffer (150 mM NaCl in 5 mM PB) at pH 7.4. The complex association constant ( $K_S$ ) and the binding stoichiometry ( $n$ ) were determined using previously reported method.<sup>21</sup>

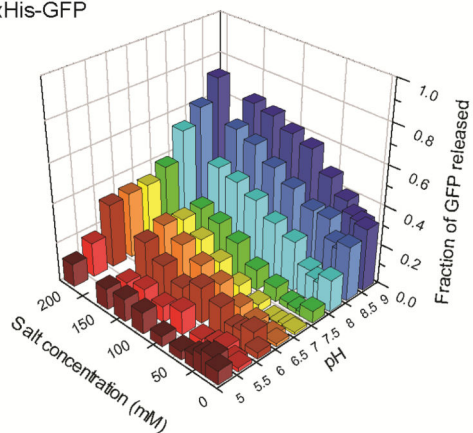
(a) 12xHis-GFP



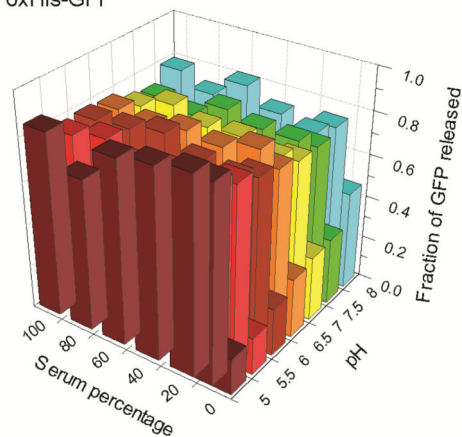
(a) 12xHis-GFP



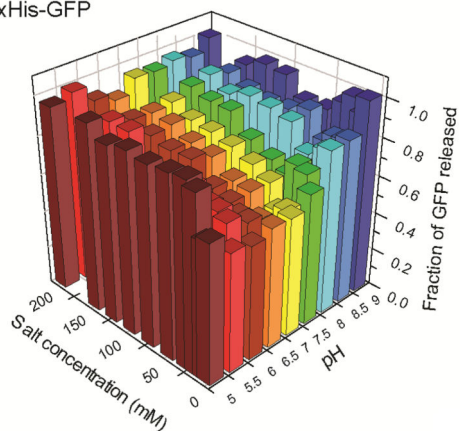
(b) 6xHis-GFP



(b) 6xHis-GFP



(c) 1xHis-GFP



(c) 12xHis-GFP

**Fig. 3.**

Responsiveness of the carboxylate-histidine zipper towards pH and salt concentration. Fluorescence titrations between 400 nM of AuNP-COOH and 100 nM of (a) 12xHis-GFP, (b) 6xHis-GFP, and (c) 1xHis-GFP were performed parametrically varied pH and salt (NaCl) concentrations in 5 mM PB. The intensity of GFP released from nanoparticles was normalized against the intensity of free GFP.

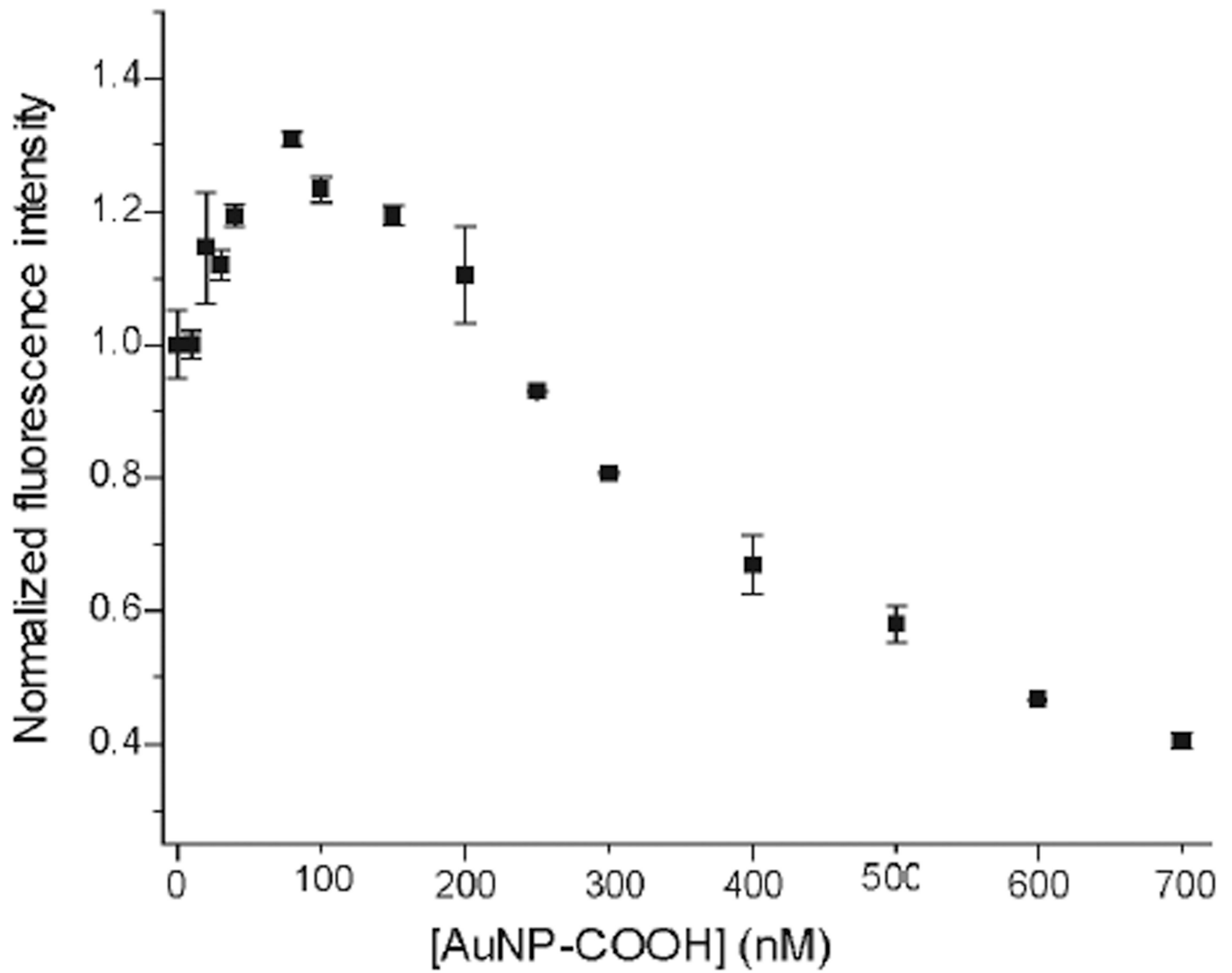


**Fig. 4.** Reversible carboxylate-histidine zipper formation between AuNP-COOH and (a) 12×His-GFP, and (b) 6×His-GFP at serum conditions. 400 nM of AuNP-COOH was titrated against 100 nM of His-tagged GFPs varying the serum percentage and pH at 150 mM salt (1×PBS) concentration. (c) Fluorescence titrations between AuNP-COOH and 12×His-GFP (100 nM) at 55% serum condition, pH 7.4.